Review

Journal of
Nanoscience and Nanotechnology
Vol. 20, 1–20, 2020
www.aspbs.com/jnn

AMERICAN SCIENTIFIC PUBLISHERS
Copyright © 2020 American Scientific Publishers
All rights reserved
Printed in the United States of America

Ultrasound-Mediated Drug Delivery in Cancer Therapy: A Review

Nour M. Al Sawaftah and Ghaleb A. Husseini*

Department of Chemical Engineering, American University of Sharjah, Sharjah, United Arab Emirates

The use of ultrasound as a medical diagnostic tool began in the 1940s. Ever since, the medical applications of ultrasound have included imaging, tumor ablation, and lithotripsy; however, an ever-increasing body of literature demonstrates that ultrasound has potential in other medical applications, including targeted drug delivery. Site-specific drug delivery involves delivering drugs to diseased areas with a high degree of precision, which is particularly advantageous in cancer treatment as it would minimize the adverse side effects experienced by patients. This review addresses the ability of ultrasound to induce localized and controlled drug release from nanocarriers, namely micelles and liposomes, utilizing thermal and/or mechanical effects. The interactions of ultrasound with micelles and liposomes, the effects of the lipid composition, and ultrasound parameters on the release of encapsulated drugs are discussed. In addition, a survey of the literature detailing some *in vitro* and *in vivo* ultrasound triggered drug delivery systems is presented.

Keywords: Ultrasound, Micelle, Liposome, Targeted Delivery, Cavitation.

CONTENTS

1. INTRODUCTION

1.1. History of Ultrasound

Ultrasonics is a branch of acoustics that focuses on vibratory waves of frequencies higher than the audible range, i.e., greater than 20 kHz [1]. The first detailed experiments proving the existence of non-audible sound waves were conducted in 1794 by the Italian physiologist Lazzaro Spallanzani. Spallanzani studied the flight behavior of bats and concluded that they could navigate using sound rather than sight, a phenomenon known as echolocation [2]. Ultrasonics, as an independent field of study, was established during World War I when technologies using ultrasound (US) waves were developed to detect enemy vessels. The first working sonar system was designed and built in the United States by the Canadian inventor Reginald Fessenden in 1914. Later, the French physicist Paul Langévin and Russian scientist Constantin Chilowsky developed a powerful high-frequency ultrasonic echo-sounding device which they called the 'hydrophone' [3, 4].

The use of US as a medical diagnostic tool began in 1942 when Karl Dussik, a neurologist at the University of Vienna, attempted to locate brain tumors by measuring the transmission of US beams through the head. John Julian Wild, an English physician, laid the foundations of ultrasonic tissue diagnosis with his publication on amplitude mode (A-mode) US investigations of intestinal and breast malignancies in 1955. Another notable figure in the development of medical US is Professor Ian Donald. Having gained initial experience in radar and sonar techniques while serving in the royal air force during World War II, Ian Donald and co-workers used US to differentiate cystic

*Author to whom correspondence should be addressed.

and solid abdominal masses leading to the publication of their findings in the Lancet in 1958 [2, 4]. Since then, this field has garnered extensive attention.

1.2. Physics of Ultrasound

US waves are mechanical sound waves with frequencies too high for the human ear to detect [5]. Within a single phase, be it gas, liquid or solid, the sound wave velocity c is dependent upon the medium's elasticity K and density ρ.

$$c = \sqrt{\frac{K}{\rho}} \tag{1}$$

The frequency of a sound wave is defined as the number of oscillations (or vibrations) per second and is measured in Hertz *Hz*. The wavelength λ describes the distance traveled in one oscillation and is derived from the frequency and the velocity [1, 5].

$$\lambda = \frac{c}{f} \tag{2}$$

The amplitude of a wave, A, can be measured in units of length or pressure. In terms of length, the amplitude is the maximum displacement of a point on a vibrating body or wave measured from its equilibrium position, whereas in terms of pressure, the amplitude describes the maximum local pressure [1, 5, 6].

In an ideal elastic medium, none of the kinetic energy of the passing wave would be dissipated as heat; however, real-life media do not behave ideally, meaning that, as a wave passes through a medium, some of its energy is lost as heat in a process known as attenuation.

Attenuation is caused by the reflection, refraction, scatter, and absorption of waves. Reflection is the change in the direction of a wave at an interface between two different media, while refraction is the deflection of a wave from its original direction as it passes between tissues with different acoustic properties. The acoustic property defining the difference between tissues is acoustic impedance Z, expressed mathematically as [1, 5, 7]:

$$Z = \rho c \tag{3}$$

Scatter occurs when a wave encounters a structure much smaller than its wavelength, while absorption is the conversion of sound energy into heat and is considered the main source of sound wave attenuation [1, 5, 7]. Attenuation is measured in relative units based on the intensity of the sound energy along the propagation path [1, 5, 7].

$$I_x = I_0 \exp(-2\alpha x) \tag{4}$$

Here I_x is the local intensity at distance x from the source, I_o is the initial intensity at the source, and α, which is a function of frequency, is the absorbance coefficient [8, 9].

1.3. Generation of US Waves

In most applications, US waves are generated by a transducer containing a piezoelectric crystal. Piezoelectric crystals convert electrical energy (electric current) to

Nour M. Al Sawaftah received her Bachelor of Science degree in Chemical Engineering in 2016 and a Master of Science degree in Biomedical Engineering in 2019 under the guidance of Dr. Ghaleb Husseini working at the American University of Sharjah (AUS), Sharjah, UAE. Her thesis focused on ultrasound enhanced release of transferrin coupled liposomes as drug delivery carriers in cancer treatment. Currently, she joined the Drug Delivery Laboratory at AUS as a research assistant.

Ghaleb A. Husseini is a Professor of Chemical Engineering at the American University of Sharjah. He works in the area of ultrasonic drug delivery. He has over 150 academic publications, one patent (3 more filed) and three book chapters, and is cited over 3700 times. According to Google Scholar, he holds an h-index and i10-index of 33 and 51. respectively. He held the distinguished lecturer position at IEEE-EMBS for two years and his project was highly commended by ICHEME in 2016. He is currently serving on the editorial board of the International Review of Applied Sciences and Engineering (IRASE) and as an Associate Editor for IEEE-Transaction on Nanobioscience (IEEE TNBS). He formed the 'Ultrasound in Cancer Research' Group at the American University of Sharjah in 2012, leading a team of undergraduate and graduate students, faculty members, and visiting intellectuals. He has also set up a biomedical engineering lab at AUS to aid the project. As a response to the successes of the team, he has been interviewed and his work highlighted by a number of local and international newspapers, as well as key television channels.

mechanical energy (sound waves) and vice versa. When an electrical pulse is applied to the crystal, it vibrates, pushing and pulling the air surrounding it, and producing an US wave in the process. In turn, when US waves strike an object and are reflected back to the transducer as echoes, the crystal converts this mechanical pulse to an electrical signal [10]. Alternatively, US waves can be generated using magnetism, a phenomenon known as magnetostriction. In this case, a magnetostrictive crystal changes its dimensions in response to an applied magnetic field, thereby producing ultrasonic waves. Moreover, US can be produced using a whistle or siren-type generator. In this method, gas or liquid streams are passed through a resonant cavity, causing ultrasonic vibrations characteristic of the particular gas or liquid [11, 12].

1.4. Medical Applications of Ultrasound

US in medical applications can be divided into either low- or high-intensity. Low-intensity US is generally used in diagnostic applications meant to obtain information about the state of tissues and organs, e.g., imaging. The US energy deposition, in this case, is intended to be minimal so as not to produce any biological effects. On the other hand, high-intensity US is aimed at manipulating matter and therefore finds more usage in therapeutic purposes where the deposited energy is intended to create a biological effect, be it mild such as healing in physical therapy or more extreme and destructive, such as the ablation of tumors [1, 11, 13]. US imaging (also known as ultrasonography) is achieved by transmitting a burst of acoustic energy from the US transducer. The US pulse then propagates as a wave through the tissues and can be reflected or refracted at different tissue boundaries. In general, at a certain intensity, the higher the frequency, the higher the imaging resolution; however, this is at the expense of lower penetration [1, 12, 14]. An advanced application of ultrasonography is Doppler sonography. The Doppler effect exploits the fact that a shift in frequency and amplitude occurs between a wave leaving the transducer and the wave received after being reflected from a moving object. Doppler sonography applies the concept of the Doppler effect to measure blood flow in different parts of the body [1, 14]. Other medical applications of US include lithotripsy, which involves the use of focused US to break up kidney stones, and focused ultrasound (FUS) surgery which requires the use of high intensity focused ultrasound (HFIU) to generate highly localized heating to treat cysts and tumors [14].

1.5. Biological Effects of Ultrasound

In therapeutic applications, the biological effects of US on tissues and cells can be either thermal or mechanical. The three primary mechanisms by which US waves induce these bio-effects are thermal, cavitational, and acoustic streaming. Krasovitski et al. [15] proposed an additional, non-thermal, non-cavitational interaction mode called the bilayer sonophore effect.

1.5.1. Thermal Effects

The thermal effect of US is primarily an increase in the medium's temperature due to the absorption of energy from US waves. The rate of heat generated by US waves is directly proportional to the frequency of the waves and exposure time and is inversely proportional to the specific absorption coefficient of the targeted tissue. Consequently, the higher the medium's absorption coefficient, the more significant the increase in temperature, and in turn, the thermal effect experienced by the tissue [15, 16].

1.5.2. Cavitational Effects

Acoustic cavitation can be best defined as the formation, growth, oscillation, and collapse of gas-filled cavities in a fluid medium due to induced pressure changes (refer to Fig. 1). The sources of the gas bubbles or cavitation nuclei are usually pre-existing bubbles that were present in the fluid, or bubbles that were formed when the pressure was reduced below the vapor pressure of the liquid. The pressure change caused by the passage of an US wave through the insonated medium leads to the formation of such bubbles, an event referred to as cavitation. There are two main types of acoustic cavitation: stable and inertial (transient) cavitation. In stable cavitation, the bubble's radius varies about an equilibrium value; in contrast, inertial cavitation bubbles grow rapidly, expanding to twofold or threefold their resonant size (limiting value), and then collapse violently [17, 18]. The growth of cavitating bubbles in an US field is aided by a process called rectified diffusion, where the net amount of gas diffusing into a bubble during its expansion is greater than that diffusing out of it during its contractile stage. During inertial cavitation, the collapse of bubbles produces momentary surges in local temperature and pressure. The vicinity of these cavitation spots has

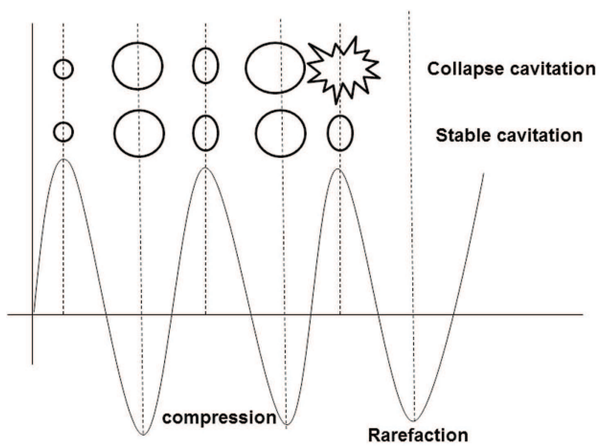

Figure 1. Transient and stable cavitation.

been shown to reach temperatures of 5000 K and pressures of 1000 atm. In addition, the bubble collapse creates shock waves that propagate and cause structural shifts in the surrounding tissues by micro-jets. Although stable cavitation bubbles can cause damage to biological tissues, it is widely accepted that the primary mechanism for the structural alteration of cells is transient cavitation [1, 16, 19].

Cavitation does not occur until certain conditions have been met; the factors that determine whether cavitation will occur or not are [1, 15, 16]:

- US intensity: Cavitation does not happen at all intensities; for a particular bubble size, there is a threshold intensity beyond which transient cavitation occurs. The threshold intensity tends to increase with increasing US frequency, ambient pressure, medium viscosity, and ion concentration. In contrast, the threshold intensity decreases with elevated medium temperatures and gas content. Therefore, transient cavitation is more frequent at low frequencies. Apfel and Holland [1] introduced a Mechanical Index (MI) that can act as an indicator of the possibility of occurrence of transient cavitation in an insonated medium. The MI is mathematically defined as follows:

$$\mathrm{MI} = \frac{P_{\mathrm{neg}}}{\sqrt{f}} \tag{5}$$

Where P_{neg} is the maximal negative pressure, in MPa, and f is the frequency in MHz. When MI > 0.7, there is a high possibility that transient cavitation will occur. Apfel and Holland also showed that for ultrasonic frequencies below 1 MHz, an acoustic pressure threshold of around 0.2 MPa is sufficient to initiate transient cavitation in aqueous solutions and blood.

- The number and availability of cavitation nuclei: The likelihood of cavitation occurrence increases with an increased number of nuclei available, which are common in non-degassed water, but are rare in animal tissues.
- The availability of physical space for bubbles to form and grow: Intact cells and extra-cellular matrices do not have the dimensions and preexisting nuclei to support cavitation. On the other hand, blood vessels possess both the dimensions and cavitation nuclei needed for the initiation of cavitation when a high enough US pressure field exists.

1.5.3. Acoustic Streaming Effect

When US waves with high amplitudes are used to insonate a medium, a transfer of momentum from the US wave to the medium may lead to the generation of unidirectional flow currents in the fluid, a phenomenon known as acoustic streaming. The velocity of the stream is directly proportional to the attenuation coefficient of the medium, the US intensity, and the surface area of the transducer and is inversely proportional to the speed of sound in the medium in question and the bulk viscosity. The leading cause of acoustic streaming is US reflection and other distortions that take place during wave propagation. So far, the clinical value of acoustic streaming has only been minimally explored [1, 15, 16]. Figure 2 depicts acoustic microstreaming and the formation of micro-jets.

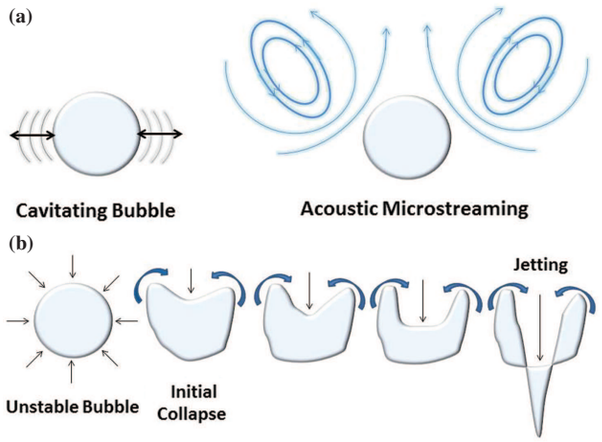

Figure 2. Schematic diagram of (a) acoustic microstreaming, and (b) the formation of micro-jets.

1.5.4. Bilayer Sonophore Effect

This model is based on the direct effect US waves have on bilayer membranes. The ultrasonic pressure wave fluctuates between positive (compression) and negative (rarefaction) values. At the negative pressure stage, the space between the membrane bilayers tends to increase while at the positive pressure phase, the spacing decreases. As a result, the continuity of the membrane is briefly interrupted, and fenestrations through which substances can be transported across the plasma membrane are created. The authors of this theory intended for the bilayer sonophore effect to be an explanation of the non-thermal effects of US at intensities below the threshold [15].

1.6. Ultrasound Sonochemistry

When an US wave passes through a liquid, it creates collapsing cavitation bubbles; the vicinity of these cavitational bubbles is characterized by high temperature, high atmospheric pressure, rapid heating, and cooling rates, as well as the formation of some oxidants of hydroxyl radicals, hydrogen peroxide, ozone etc. Chemical reactions involving acoustic bubbles are referred to as sonochemical reactions [20]. The unique environment created by cavitating bubbles provides a new route for chemical reactions that is difficult to achieve under normal conditions. For instance, bubble collapse can cause polymers or macromolecules to stretch and their coils to open. These macromolecules are then broken by shock waves created as a result of the final collapse of cavitating bubbles; this is referred to as shear degradation by US, which is depicted in Figure 3. In addition to shear degradation, macromolecules may

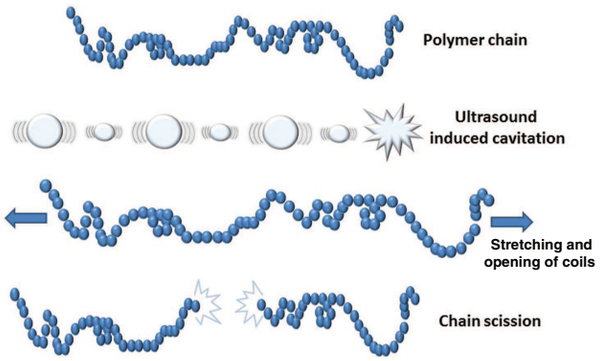

Figure 3. Mechanism of ultrasound-induced polymer chain scission.

be broken down by US due to the production of OH radicals [21, 22].

1.7. Micelles

Micelles are biocompatible, core–shell structures varying in size from 50 to 200 nm (Fig. 4). They are made up of amphiphilic molecules such as lipids or polymers. When exposed to an aqueous environment, the component molecules of the micellar systems arrange themselves in spheroidal structures with the hydrophobic cores hidden inside the structure, while the hydrophilic groups would be directed outwards. Drugs can be loaded into micelles either through chemical covalent bonding or through physical encapsulation. Poorly water-soluble drugs tend to be loaded into the micelle's hydrophobic core, whereas hydrophilic drugs tend to align themselves near the hydrophilic components of the micellar structure. Micelles have proven to be remarkably smart drug delivery systems (SDDSs) due to their ease of preparation, high stability under physiological conditions, efficient and versatile loading capacity, controlled release kinetics, and the possibility and ease of functionalization. Various cancer-related drugs such as paclitaxel, doxorubicin (DOX), 5-fluorouracil, cisplatin, triptorelin, and xanthone have been successfully encapsulated into micelles [23–26].

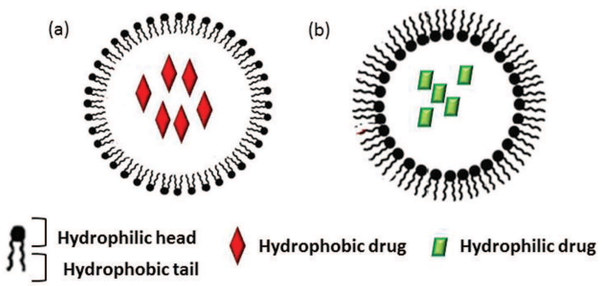

Figure 4. Schematic of the structure of polymeric micelles (a) in a polar solvent, (b) reverse micelles in a nonpolar solvent.

1.8. Liposomes

Liposomes are nanosized to microsized artificial vesicles composed of the same materials that make up the cell membrane, i.e., cholesterol, nontoxic surfactants, and natural phospholipids. The name liposome is derived from the Greek words 'Lipos' meaning fat and 'Soma' meaning body. Liposomes were first discovered in 1961 by British hematologist Dr. Alec Bangham while studying the effects of phospholipids on blood clotting. Ever since their discovery, liposomes have found numerous applications in several scientific disciplines [27, 28].

Structurally, liposomes are concentric spheres of phospholipid bilayers separated by aqueous compartments (Fig. 5). When amphipathic phospholipids are exposed to water, they tend to reassemble into tiny spheroidal structures that are either bilayered or monolayered. The monolayered structures are micelles, while the bilayer structures are liposomes [27]. Liposomes are structured in such a way that both outer surfaces are comprised of the hydrophilic head groups, whereas the hydrophobic tails are directed opposite to each other, forming the inner part of the structure [29–31].

1.8.1. Classification of Liposomes

Liposomes can be classified based on structure, method of preparation, and composition. With respect to structural parameters, liposomes are categorized as unilamellar, small unilamellar, medium unilamellar, large unilamellar, giant unilamellar, oligolamellar, multilamellar, and multi-vesicular vesicles [27, 32]. Based on composition, liposomes are classified into conventional, fusogenic, pH-sensitive, cationic, long circulatory, and immunoliposomes.

The choice of liposomal preparation method relies on several factors, such as the physicochemical properties of the liposomal ingredients, the material to be encapsulated,

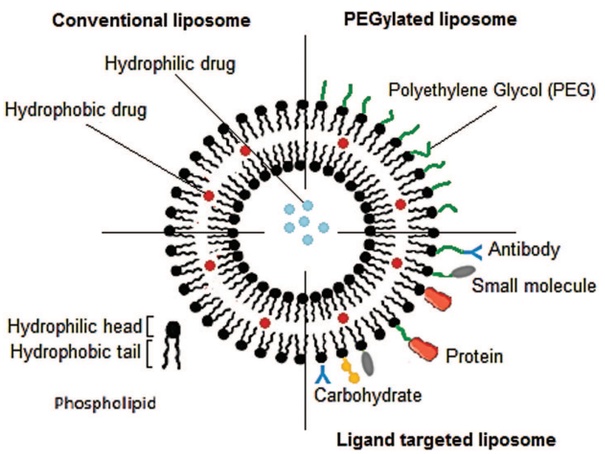

Figure 5. Schematic of the conventional and functionalized liposome structure.

the nature of the medium in which the lipids will be dispersed, as well as the concentration of the entrapped substance and its potential toxicity. All methods of preparing liposomes involve the following four steps [33]:

1. Drying down the lipids by evaporating the organic solvent.
2. Dispersing the lipids in an aqueous medium.
3. Purifying the resultant liposomes.
4. Analyzing the final product.

The entrapped agents can be loaded into the liposomes either before or during the formulation process (passive loading); certain compounds, which display both water and lipid solubility, can be introduced into the liposomes after the formation of the vesicles (remote or active loading). Consequently, the techniques for preparing liposomes are divided into passive and active loading methods.

1.8.2. Surface Functionalization

Nanocarriers with long-circulating properties have garnered considerable attention in biomedical fields, particularly in applications such as blood pool imaging and targeted drug delivery. Applications that require an increased circulation-time require nanocarriers to evade detection by the reticuloendothelial system (RES) and clearance by the organs of the mononuclear phagocyte system (MPS). This desired "invisibility" can be achieved by decorating the surfaces of nanoparticles (NPs) with stealth-imparting polymeric substances that suppress opsonization and the subsequent uptake by macrophages. Such NPs are referred to as stealth NPs [34, 35]. Surface modification of NPs with polymeric substances can be performed in one of three ways [36]:

1. The physical adsorption of the polymer onto the surface of the NPs.
2. The incorporation of the agent during NP preparation.
3. The covalent attachment of the reactive groups onto the surface of pre-formed NPs.

Other than developing macrophage-resistant properties, grafting NPs with polymeric substances enhances their surface stability. The presence of such surfactants significantly reduces the attractive Van der Waals forces between approaching particles; moreover, elastic and osmotic factors play a role in increasing the repulsive barrier between the NPs. This elastic contribution results from a loss of the conformational freedom of the polymeric chains, and since the available volume for each polymer group is reduced, the particles are forcedly separated. On the other hand, the osmotic pressure contribution arises from an increase in the polymer density on the nanocarrier surface, causing an influx of water to the region and forcing the particles apart [37].

Several natural and synthetic materials have been investigated for developing stealth NPs, including dextrans, pullulan, and gangliosides [34, 35]. However, polyethylene glycol (PEG) lipopolymers have brought about the most significant breakthrough in the development of stealth technologies. The presence of PEG on the surface of nanocarriers extends their blood circulation time while reducing their uptake by the RES, which leads to improving the distribution of the carriers in perfused tissues. The presence of PEG also helps reduce vesicle aggregation, thus enhancing the stability of the formulations [35]. PEG is a synthetic, linear polyether diol that exhibits high biocompatibility, low immunogenicity, ease of synthesis, high flexibility, and aqueous/organic solubility. The fact that PEG is soluble in organic media facilitates the synthesis of PEGylated lipids and the formulation of stealth NPs. The PEG segment may be synthesized with molecular weights varying between 400 to 50,000 Da [38]. The molecular weight, along with the grafting density, is essential in determining the conformation of PEG and the steric suppression of the opsonization process. Brush-like PEG conformations dominate at high PEG grafting densities, whereas the mushroom conformation is more common at low grafting densities. PEG-based lipopolymers consist of a PEG segment of variable lengths or configurations

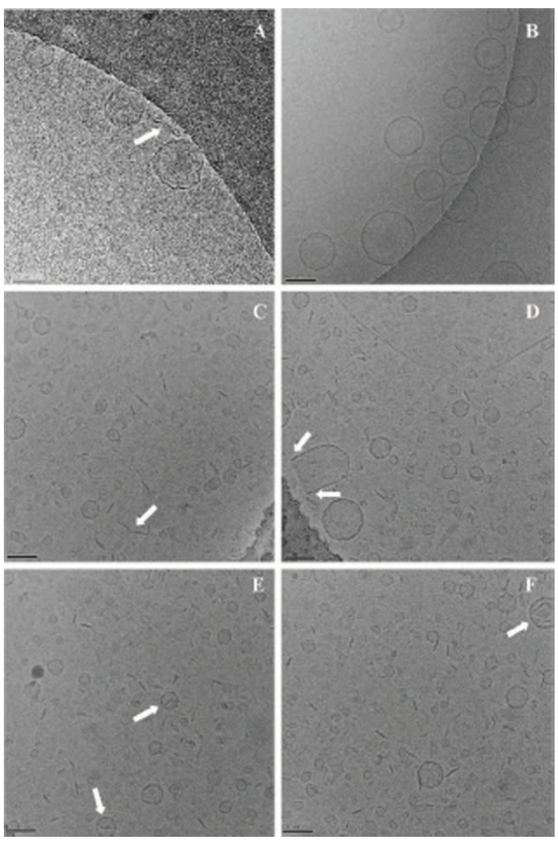

Figure 6. Cryo-TEM images of (A) DPPC MLV after 20 min of FUS (B) DPPC MLV passed through polycarbonate filters of 200 nm pore; (C–F) DPPC/LysoPC/DSPE-PEG-2000 MLV after 20 min FUS. Reprinted with permission from [47], Tejera-Garcia, R., et al., **2011**. Making unilamellar liposomes using focused ultrasound. *Langmuir*, *27*(16), pp.10088–10097. Copyright@American Chemical Society.

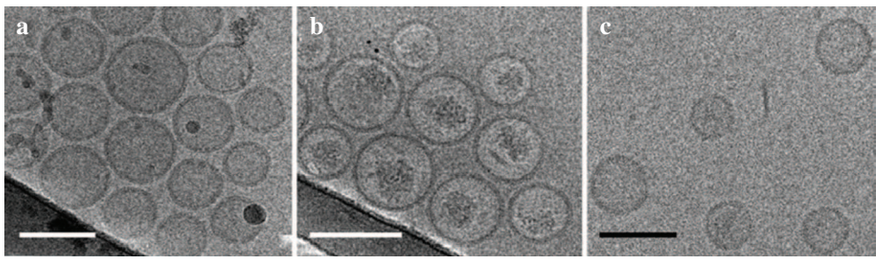

Figure 7. Cryo-transmission electron microscopy images of (a) liposomes before remote loading of MPS, (b) liposomes after remote loading of MPS, and (c) liposomes remote loaded with MPS after being exposed to LFUS. Reprinted with permission from [49], Schroeder, A., et al., **2007**. Controlling liposomal drug release with low frequency ultrasound: Mechanism and feasibility. *Langmuir*, *23*(7), pp.4019–4025. Copyright@American Chemical Society.

attached to the lipid (acyl) moiety via a linker, e.g., phosphate ester, carboxylate ester, or an amide bond. The acyl group is a determining factor of the physical state of the lipid assemblies, whether they are lamellar or micellar, and controls the extent of PEG lipopolymers' inclusion into the nanocarrier's membrane. In addition, the choice of the linker directly influences the behavior of the modified NPs; for instance, ester linkages are highly susceptible to decomposition in biological media whereas phosphate linkers may incite opsonization [34, 39].

1.9. Ultrasound-Guided Drug Delivery

Ultrasound-guided drug delivery is a promising approach to treat certain types of cancer because the technology is noninvasive, readily available, and permits the spatially confined delivery of drugs to targeted areas with a high degree of precision, thus minimizing the adverse effects on healthy tissues. The US-responsive nanocarrier system can be designed to respond to the thermal effects of US, mechanical effects of US, or a combination of both [40].

1.9.1. Using Ultrasound to Form Micelles and Liposomes

The word micelle was first introduced into the scientific literature in 1858 by the Swiss botanist Karl Wilhelm von Nägeli. The word micelle originates from the Latin word "mica" meaning crumble, and Karl von Nägeli coined this term to describe the crystalline aggregates of starch and cellulose molecules that formed in water. The term "micelle" next appeared in James Willian McBain's discussion contribution, entitled: "on the mobility of highly-charged micelles," at the 1913 Faraday meeting. McBain used the term to describe aggregates of soap molecules in aqueous solution [41]. The first model of spherical micelles, which is still used today, was proposed by G.S. Hartley. In Hartley's model, the polar headgroups form the exterior of the aggregate, and the hydrophobic moieties form the interior [42]. In the early 1960s, Saunders et al. [43] discovered that exposing aqueous lecithin dispersions to US resulted in the formation of what was then believed to be "lecithin micelles." At that point, the discovery had not been made yet that these micellar structures were, in fact, unilamellar vesicles with an aqueous inner core. Later, Papahadjopoulos et al. [44, 45] showed that phospholipid suspensions exposed to low-frequency US (LFUS) also led to the formation of such small unilamellar vesicles (SUVs). However, it was Huang and coworkers [46] who first studied these SUVs carefully. Their work involved the separation of phosphatidylcholine vesicles, formed by ultrasonic irradiation, using molecular sieve chromatography on large pore aerosol gels. These studies led to an improved understanding of liposomes, including their phospholipid bilayer structure, liposomal dimensions, and the asymmetric lipid distribution between the inner and outer layers of the SUV bilayer [1]. In later studies, it was discovered that different phospholipid formulations exposed to similar LFUS conditions resulted in differently sized liposomes; and that for a given phospholipid formulation, the longer the exposure to US irradiation the smaller and more homogeneous the liposomes.

Another application of US in micelle and liposome formation is the disruption of multilamellar vesicles (MLV) to produce unilamellar vesicles (ULV). Lipid vesicles form spontaneously when phospholipids are dispersed in an aqueous solution. In the early stages of vesicle formation, the hydrated lipid sheets detach by agitation and close to form large MLVs. This formation prevents contact between water and the hydrophobic core of the bilayer. Once MLVs have formed, any reduction in size requires energy. Several methods can be employed in this step, one of which involves the disruption of MLVs using US. These approaches produce SUVs almost exclusively, and the most common instruments for the preparation of vesicles using US are bath and probe type sonicators [47]. Although both types of sonicators use low frequencies and unfocused energy outputs; bath sonicators are favored because probe sonicators may shed some metal particles into the sample which need to be removed by centrifugation [47, 48].

Two mechanisms have been proposed to explain the formation of vesicles by sonication, the first, is the excision of smaller vesicles from the MLV surface due to the energy of the acoustic pressure waves produced by US, while the second is the breaking down of larger MLVs

into small phospholipid bilayer fragments (PBF), which then re-assemble into liposomes [1, 47, 48]. Richardson et al. [18] attempted to explore the role of cavitation in liposome size formation. Aqueous lipid suspensions surrounding a hydrophone were exposed to various US intensities, and hydrostatic pressures, the size distribution of these lipid suspensions was then measured using dynamic light scattering (DLS). Experiments showed that increasing the US intensity at atmospheric pressure decreased the average liposome diameter, and that increasing hydrostatic pressure inhibited the presence of collapse cavitation. Therefore, collapse cavitation did not correlate with decreases in liposome size, and any reductions in size were attributed to stable cavitation. Moreover, a mathematical model was developed based on the Rayleigh-Plesset equation of bubble dynamics; this model was used to predict the US intensities and pressures needed to create shear fields sufficient to cause the size of liposomes to change. The results obtained using this model correlated well with the experimental data.

1.9.2. Controlled Release of Drugs from Micelles and Liposomes Using Ultrasound

As mentioned earlier, an optimal nanocarrier formulation is expected to accumulate intact at the target site and then release its contents at a controlled rate. The release of the nanocarrier's payload can be in response to either internal or external stimuli. This review focuses on drug release triggered by an external acoustic stimulus, namely US [49]. Controlled drug release from liposomes using US involves the disruption of the liposomal structure and the subsequent release of the payload in response to either an elevation in temperature or mechanical effects produced by US. Conventionally, liposomes are stable in the physiological temperature range, as they are usually made up of lipids with phase transition temperatures in the range of 40–45 °C. When an ultrasonic beam is focused on a particular area of the body, the temperature in that region may rise beyond the transition temperatures of the lipids, interrupting the orderly packing of the lipid bilayer and introducing free volumes into the structure which allow the drug to move freely from the liposomal core to the extra-liposomal medium [1, 16].

In contrast to liposomes, drugs encapsulated inside micelles are located in the inner hydrophobic core that is held together by hydrophobic interactions, which become stronger with increasing temperature. Therefore, a different approach is needed to impart temperature responsiveness to micelles. One approach to address this issue involves incorporating thermo-responsive blocks to the micellar structure; lower critical solution temperature (LCST) polymers, such as poly(N-alkylacrylamide) compounds, were investigated as components of temperature-responsive micelles. A different approach to developing thermo-sensitive micelles entails the polymerization of temperature-responsive LCST hydrogels inside micellar cores [21]. A particularly innovative method was established by Hennink's group [50]. In their work, a copolymer was synthesized with PEG as the hydrophilic block, and a temperature-responsive LCST fragment as the hydrophobic block, the hydrolysis of the pendant side groups in the hydrophobic block converted it into a hydrophilic block, which resulted in micelle dissolution and drug release.

The mechanical effect of US-mediated drug release is manifested in the form of sonoporation, where sound energy is used to enhance the permeability of plasma membranes through the creation of pores. Both stable and transient cavitation can bring about the process of sonoporation. Stable cavitation can create pores by altering vascular permeability and hence improving the delivery to the whole targeted tissue. In contrast, inertial cavitation affects the permeability of individual cells for the improved delivery of payloads at that level. Studies found that transient cavitation can increase drug release in a more substantial manner because it induces additional mechanical effects, i.e., shockwaves and micro-jets that further enhance the effects of sonoporation. Sonoporation was first described by Fechheimer et al. [51], who exposed cell suspensions of live slime mold amoebae to US in the presence of fluorescein-labeled dextrans. Live slime mold amoeba is normally impermeable to dextrans due to their size; however, the exposed cell samples were found to have around 40% uptake of the fluorophore, and the process was subsequently reproduced in mammalian cells (DNA delivering). US-mediated drug delivery is considered a safe route which allows for the delivery of therapeutics without compromising the body's physiological barriers, as the cell membrane permeabilization is reversible, with the membranes usually returning to their original configurations within a short period of time [1, 16, 40, 52].

The pioneering work in the field of US-mediated micellar drug delivery was done by Pitt, Rapoport, Husseini et al. [53]. In 1997, Rapoport and Pitt [54] investigated US-triggered drug delivery from Pluronic P-105 polymeric micelles. They discovered that the combination of US and micelles could decrease the effective dosage of chemotherapeutics which in turn helped reduce the systemic side effects associated with the high doses of chemotherapeutic agents usually administered to cancer patients. In another study, Pitt, Husseini, and Kherbeck [55] examined the application of low-frequency US (LFUS) to trigger the release of DOX from folate-conjugated Pluronic P105 micelles. The results showed that the percent drug release increases with increasing US power intensity; the maximum amount of release was 14%, which was measured at 5.4 W/cm^2. Stevenson-Abouelnasr et al. [56] studied the release mechanisms and release kinetics of DOX from Pluronic P105 micelles exposed to US. The mechanisms proposed to explain the release of DOX from micelles upon insonation, and its subsequent re-encapsulation when

the sonication is stopped include micelle destruction, destruction of cavitating nuclei, reassembly of micelles and the re-encapsulation of DOX. Moreover, the proposed kinetic model was solved numerically for an insonation period of 60 s and compared against the experimental drug release data, values for the constants appearing in the model were determined using the best fit to the experimental data. The model was found to be an excellent fit to the experimental data, and a close agreement was achieved for each phase of the release. Xia et al. [57] proposed the concept of high intensity focused US (HIFU) mediated release from polymeric micelles. The release mechanism was based on chain scission (the degradation of the main polymer chain), the chemical disruption of micelles, and the irreversible release of the payload.

With regard to US-mediated liposome drug release, one of the earliest experiments was conducted by Tacker and Anderson [58]. Transitional cell carcinoma (TCC) tumors were transplanted into the hind legs of C3H/Bi mice. Prior to the delivery of the liposomal treatment, the tumors were heated to 42 °C (using US), the animals were then injected with methotrexate (MTX)-encapsulating liposomes. The tumors were then removed, and the MTX uptake of each tumor was noted and compared to the controls, i.e., unheated tumors. Heated TCC tumors showed an 11.9-fold increase in MTX uptake compared to non-heated tumors receiving the same dose, while animals receiving free MTX did not exhibit a temperature-dependent difference. In 1994, Ning et al. [59] showed a six-fold increase in DOX release from stealth liposomes by inducing hyperthermia using an US apparatus and a heating bath system. Schroeder et al. [49] used low-frequency (20 kHz) US to trigger the release of three different encapsulated drugs: methylprednisolone hemisuccinate, DOX, and cisplatin. Up to 180 s of US exposure demonstrated the release of nearly 80% of the drug from liposomes, independent of the drug or method of drug loading.

Somaglino et al. [60] investigated the ability of HIFU to induce liposomal drug release by inertial cavitation in animal and *in vitro* models. The AT2 phenotype of the Dunning R3327 rat prostatic carcinoma was used, and the tumor cells were subcutaneously injected into Copenhagen male rats. Controlled cavitation at 1 MHz was applied to the tumors 48 hours after liposome injection; the *in vitro* study provided the suitable US parameters for inducing cavitation safely in liposomal drug release. However, when studying the *in vivo* model, a small non-significant therapeutic effect of US-liposomal treatment was observed compared to liposomes alone. Moreover, Mannaris et al. [61] investigated the localized drug-delivery of DOX-loaded thermo-sensitive liposomes with US-induced hyperthermia. The acoustic conditions were derived theoretically then validated experimentally, and around 80% DOX release was achieved after 15 min of hyperthermia at 43 °C.

In another study, Gray et al. [62] conducted a phase I trial study involving focused US–mediated hyperthermia-triggered drug delivery to solid liver tumors. The ten participants were treated from March 2015 to March 2017 using a clinically approved focused US system to release DOX from thermo-sensitive liposomes. For all participants, CT images were used to monitor the progress of the treatment. Furthermore, a model of US-induced hyperthermia was developed using the participants' data and finite element calculations to specify the US parameters and to estimate temperature fields for each test subject. The feasibility of this treatment was confirmed based on the negligible mean difference between the model-predicted and actual focused US powers required to achieve hyperthermia-mediated drug delivery, whereas the safety was tested and confirmed based on the lack of focused US–related adverse effects. The model-based treatment planning approach was verified by comparing the model and thermometry results. The model-prescribed treatments resulted in similar levels of enhanced drug delivery with or without real-time thermometry. These outcomes suggest that it may be feasible to pair planning models with monitoring techniques to guide and ensure the safety of US-induced hyperthermia treatments. Table I presents a summary of relevant studies that utilized US to release drugs from both micelles and liposomes. It details the tumor model or animal cancer models that were used, the anti-tumor drugs that were injected, as well as the main acoustic parameters used.

1.10. Effect of Membrane Constituents on US Drug Release from Micelles and Liposomes

Many studies reporting the use of micelles as drug carriers employed Pluronic® micelles. However, the main shortcoming in the design of Pluronic® P-105 micelles is that they tend to be unstable upon dilution; this limitation led researchers to attempt various methods to stabilize P-105 micelles. Rapoport [63] investigated three different routes for Pluronic® micelle stabilization. The first route was direct radical crosslinking of micellar cores; however, this decreased the drug loading capacity of these carriers. In the second route, vegetable oil was introduced in small concentrations into diluted Pluronic® solutions. This approach did not compromise the loading capacity of Pluronic® micelles at the same time it decreased micelle degradation upon dilution. The third route was a newly developed technique based on the polymerization of temperature-responsive LCST hydrogels in the core of Pluronic® micelles. The hydrogel phase swelled at room temperature, providing a high drug loading capacity; however, at physiological temperatures, the hydrogel collapsed, which in turn prevented the micelles from fast degradation upon dilution. This new drug delivery system was called Plurogel®. Zeng and Pitt [64] synthesized a polymeric micelle system with a hydrolysable segment

Table I. Summary of relevant *in vitro* and *in vivo* studies.

Drug loaded/contrast agent/model drug	Nanocarrier	Tumor model, Animal strain	Acoustic parameters	Mechanism of drug release	Main findings	Ref.
Methotrexate	Liposomes	Bladder transitional cell carcinoma, C3H/Bi mice	–	US-induced hyperthermia	• Heated TCC tumors accumulated 11.9-fold more MTX than non-heated tumors receiving the same dose.	[58]
Doxorubicin	Liposomes	Radiation-induced fibrosarcoma mouse RIF-1 tumor, male C3H/Km mice	Power density = 2 W/cm^2, Duration = 0–60 min	US-induced hyperthermia	• Temperature increase from 37 °C to 41 °C resulted in a six-fold increase in DOX release. • At 42 °C, the accumulation of S-DOX was about 10-fold and 2.5-fold higher than free drug and S-DOX at 37 °C, respectively.	[59]
Doxorubicin	Pluronic® P-105 micelles	Human leukemia HL-60 cells	Frequency = 80 kHz	FUS-induced cavitation	• Micellar DOX lowered DOX IC_{50} to 0.19 mg/mL.	[54]
Doxorubicin and ruboxyl	Stabilized pluronic® micelles	Human leukemia HL-60 cell line	Frequency = 70 kHz, Power density = 2.4 W/cm^2, Duration = 1 hr	US-induced cavitation	• US enhanced intracellular drug uptake from dense Pluronic micelles.	[63]
Doxorubicin	Pluronic® P-105 micelles	Human leukemia HL-60 cell line	Frequency = 20 kHz, Power density = 1.4, 14 and 33 mW/cm^2, Duration = 30 min	–	• Main factor that affected drug uptake was US power density. • US increased the intracellular drug uptake from Pluronic micelles.	[71]
Doxorubicin	Stabilized Pluronic® P-105 micelles	DHD/K12/TRb tumor cells, BDIX rats	Frequency = 20 and 70 kHz, Power density = 1 and 2 W/cm^2, Duration = 1 hr	LFUS-induced cavitation	• LFUS and encapsulated DOX reduced the tumor size compared with non-insonated controls.	[75]
Doxorubicin	Pluronic® P-105 micelles	Human leukemia HL-60 Human cells and drug-sensitive A2780 and MDR ovarian carcinoma A2780/ADR cells	Frequency = 20 kHz, 67 kHz and 1 MHz, Power density = 0.058, 2.8 and 7.2 W/cm^2, Duration = 15–30 sec	HFUS-induced cavitation	• Sonication at 1 MHz increased intracellular uptake of DOX from PBS and RPMI 1640.	[76]
Doxorubicin	Pluronic® P-105 micelles	–	Frequency = 70 kHz, Power density = varied	LFUS-induced cavitation	• Strong correlation between drug release and subharmonic acoustic emissions established.	[77]
Doxorubicin	Liposome	WiDr human colon cancer, 144 Balb/c nude mice	Frequency = 20 kHz, Power density = 3.16 W/cm^2, Duration = 30 min	LFUS-induced cavitation	• Significant synergism between encapsulated drug and US. • Synergetic effects larger for lower drug concentrations.	[78]

Table I. Continued.

Drug loaded/contrast agent/model drug	Nanocarrier	Tumor model, Animal strain	Acoustic parameters	Mechanism of drug release	Main findings	Ref.
Doxorubicin	Liposome	Murine mammary adenocarcinoma JC cell line, female BALB/c mice	Power density = 1,300 W/cm^2, PRF = 1 Hz; Duty cycle = 10%, Duration = 15–20 min	HIFU-induced hyperthermia	• *In vitro* incubation triggered release of 50% of DOX. • *In vivo* HIFU with LTSLs resulted in more rapid delivery of DOX.	[79]
Doxorubicin	Stabilized/ unstabilized Pluronic® P-105 micelles	–	Frequency = 70 kHz, Power density = varies	LFUS-induced cavitation	• DOX release at 37 °C from non-stabilized micelles was higher than that from stabilized micelles. • Both stabilized and non-stabilized micelles were perturbed by collapse cavitation to release DOX.	[80]
Doxorubicin	Pluronic® P-105 micelles	–	Frequency = 20 kHz, Power density = 0.058 W/cm^2, Duration = 60 s	LFUS-induced cavitation	• The model provided reasonably accurate predictions of experimental data.	[56]
Doxorubicin, Methylpredinisolone hemisuccinate, Cisplatin	Liposome	C26 murine colon adenocarcinoma cells	Frequency = 20 kHz, Intensity = 0–70 W/cm^2, Duration = 0–180 s	LFUS-induced cavitation	• 80% release for all 3 drugs was achieved.	[49]
Cyanine-5 (Cy-5)	PEG-poly (L-lysine iso-phthal-amide) micelles	–	Frequency = 1.1 MHz, Duty cycle = 5%, PRF = 1.67 kHz, Duration = 2 min	HIFU-induced cavitation and pH triggered release	• Micelles were stable at pH 4 and pH 5. • Micelles broke dowm at pH 6 and pH 7.4. • HIFU achieved significant micellar breakdown.	[81]
Doxorubicin and formaldehyde-releasing prodrugs	Stabilized Pluronic® micelles	–	Frequency = 20 kHz, Power density = 100 W/cm^2	LFUS-induced cavitation	• LFUS released 7–10% of doxorubicin from micelles.	[82]
Nile red (NR)	PLA-b-PEG copolymer micelles	–	Frequency = 1.1 MHz, Power = 0–200 W, Duration = 15 min	HIFU-induced cavitation	• Percentage NR release reached∼65% at a HIFU power output of 200 W.	[83]
Doxorubicin	Pluronic® P-105 micelles	–	Frequency = Several, power density = varied	–	• ANN used to capture the nonlinear dynamics of ultrasound-triggered drug release from polymeric micelles.	[84]
Cisplatin	Liposomes	Murine lymphoma J6456, BALB/c mice	Frequency = 20 kHz, Intensity = 5.9 W/cm^2, Duration = 120 s	LFUS-induced cavitation	• 70% of liposomal cisplatin released in tumors exposed to LFUS. • Less than 3% release in treatment groups not exposed to LFUS.	[85]
Pyrene	PEG-S-S-PLA micelles	–	Power = 80 W, Duration = 10 min	HIFU-induced cavitation and GSH redox triggered release	• Increasing HIFU power decreased the fluorescence emission intensity meaning that the percentage of released pyrene increased. • Under the combined effect of HIFU and GSH, the release percentage reached ∼95% in 10 min.	[86]

Table I. Continued.

Drug loaded/contrast agent/model drug	Nanocarrier	Tumor model, Animal strain	Acoustic parameters	Mechanism of drug release	Main findings	Ref.
Gd-HP-DO3A and Doxorubicin	Liposomes	VX2 cells, rabbits	Frequency = 1.2 MHz, Duration = 10 min	HIFU-induced hyperthermia	• Release of DOX and Gd-HP-DO3A was minimal at 37 °C but increased at 41.3 °C. • Highest increase in MR signals *in vivo* from the heated tumor region injected with TSLs.	[87]
Doxorubicin	Liposomes	Metastatic colorectal tumor cell line DHD/K12/TRb, BDIX rats	Frequency = 20 kHz, Intensity = 1 W/cm^2, Duration = 15 min	LFUS-induced cavitation	• Significant regression when US was applied. • Insonated tumors were smaller than liposomes-only control group. • MI = 1.22, indicating transient cavitation.	[88]
Doxorubicin	Pluronic® P-105 micelles	Breast adenocarcinoma tumors, female inbred Balb/C mice	Frequency = 28 kHz, Intensity = 0.04 W/cm^2, Frequency = 3 MHz, Intensity = 2 W/cm^2, Duration = 2.5 min	US-induced cavitation	• Dual frequency sonication improved drug release from micelles. • Increased drug uptake by tumors due to inertial cavitation.	[89]
Hydrophobic dye (NKX-1595)	Pluronic® P-105 micelles	–	Frequency = 22.8 and 490 kHz, Power = 0–17 W, Duration = 10 min	LFUS-induced cavitation	• Low-frequency US was more effective than high-frequency US in the degradation of the polymer. • Dye was released from micelles by physical acoustic effects.	[90]
Doxorubicin	Liposomes	AT2 phenotype of the Dunning R3327 rat prostatic carcinoma, Copenhagen male rat	Frequency = 1.13 MHz, Duration = 176–587 s	HIFU-induced cavitation	• 70% of drug released. • Small effect of US-liposomal treatment compared to liposomes alone.	[60]
Doxorubicin	Folated Pluronic® P-105 micelles	–	Frequency = 70 kHz, Intensity = 0.53–3 W/cm^2	LFUS-induced cavitation	• Percent drug release increased as US power intensity increased. • Maximum release (14%) was measured at 5.4 W/cm^2.	[55]
Doxorubicin	Liposomes	9L rat gliosarcoma cells, male Sprague–Dawley rats	Pressure = 0.55–0.81 MPa, PRF = 1 Hz, Duration = 5 min	FUS-induced cavitation and permeabilization	• Strong treatment effect in 7/8 animals in FUS + DOX group. • FUS + DOX survival time was 35 days, a 100%, and 72% improvement over the control and DOX-only groups.	[91]
Nile Red	NCL and CCL poly(ethylene glycol)-b-poly [N-(2-hydroxy-propyl) methacryl-amide-lactate] (mPEG-b-p(HPMAm-Lacn)) micelles	–	Frequency = 1.5 MHz, Acoustic power = 2.5, 5, 10, 20 W, Duration = 1–4 min	HIFU-induced shear forces	• High-frequency CW- and PW- HIFU was able to release up to 85%.	[65]

Table I. Continued.

Drug loaded/contrast agent/model drug	Nanocarrier	Tumor model, Animal strain	Acoustic parameters	Mechanism of drug release	Main findings	Ref.
Pyrene	ABA triblock copolymer micelles	–	Frequency = 1.1 MHz, Power = 0–150 W	HIFU and DTT redox triggered release	• The mechanism for US-induced micelle disruption is still under investigation. • PEG-PU (100%SS)-PEG/pyrene micelles with more disulfide bonds showed faster release rates than PEG-PU (50%SS)-PEG/pyrene micelles in the presence of DTT. • Under the combined HIFU/redox stimulus, the release was enhanced.	[92]
Doxorubicin	Liposomes	–	Frequency = 1.1 MHz, Duration = 20 s	US-induced hyperthermia	• 80% of the thermosensitive liposomes were activated	[61]
Perfluoropentane and Doxorubicin	Liposomes	Human prostate adenocarcinoma cells PC3, male athymic nude mice BALB/c strain	PRF = 5 MHz, Acoustic power = 3.25 W, Duration = 60 s	HIFU-induced hyperthermia	• DOX release of around 99% under hyperthermia.	[93]
Doxorubicin and [Gd(HPDO3A)(H_2O)]	Liposomes	R1 rhabdomyosarcoma tumors, female Wag/Rij rats	Frequency = 1.44 MHz, Duration = 15 min	HFUS-induced hyperthermia	• Hyperthermia-DOX treatment induced a 14.6-fold increase in tumor DOX concentration than the non-HIFU group and a 2.9-fold compared to the free-DOX group	[94]
Doxorubicin	Liposomes	C26 colon cancer cells, FemaleBalb/c mice	Duty cycle = 35%, PRF = 5 Hz, Power = 6 W, Duration = 30 min	HIFU-induced hyperthermia	• DOX and hyperthermia led to around 80% C26 killing.	[95]
Doxorubicin	Folated Pluronic® P-105 micelles	–	Frequency = 70 kHz, Power density = 3.54 and 5.43 W/cm^2,	–	• MLE-optimized filters outperformed other estimators in predicting micellar release using US.	[96]
Doxorubicin	Liposomes	C6 glioma cells, adult male Sprague–Dawley (SD) rats	Frequency = 690 kHz, Acoustic power = 0.32 W, Burst length = 10 ms, PRF = 1 Hz, Duration = 60 s	FUS-induced cavitation and permeabiliza-tion	• FUS + QD-CLs gave the strongest fluorescent signals, followed by the QD and QD-CLs groups. • FUS + DOX-CLs group suppressed glioma progression and extended animal survival time to 81.2 days.	[97]
Doxorubicin	Liposomes	4T1 mammary carcinoma cells, MCF-7 human breast adenocarcinoma cell and Human umbilical vein endothelial cells HUVECs,	Frequency = 1 MHz, Duration = 10 min,	HIFU-induced hyperthermia	• DOX from iRGD-LTSL-DOX rapidly penetrated interstitial tumor space after HIFU-triggered heat treatment.	[98]

Table I. Continued.

Drug loaded/contrast agent/model drug	Nanocarrier	Tumor model, Animal strain	Acoustic parameters	Mechanism of drug release	Main findings	Ref.
Doxorubicin	Folated Pluronic® P-105 micelles	–	Frequency = 70 kHz, Power density = 1.009–5.914 W/cm^2	HIFU-induced cavitation	• The model was in good agreement with experimental data. • DOX release increased with increasing power density. • The micelle reassembly increased with increasing power density.	[99]
O^{6}BTG-C18	Liposomes	Mouse glioma cell line SMA-497, VM/Dk mice	Pressure = 0.28–0.55 MPa, PRF = 1 Hz, Burst length = 10 ms, Duration = 180 s	LIFU-induced cavitation	• Tumor regression and increased survival in the LIFU- LP-O^{6}BTG-C18 glioma-bearing mice group.	[100]
Doxorubicin	Liposomes	Rat pancreatic ductal adeno-carcinoma (PDAC) cell line DSL-6A/C1, male Lewis rats (LEW/CrlBR) and female nude mice (NMRI-Foxn1nu/nu)	Frequency = 1.1 MHz	FUS-induced cavitation	• US-L-DOX group exhibited slower tumor-growth than the control, and US-alone groups.	[101]
Doxorubicin	Liposomes	Human breast cancer cells MDA-MB-468 and MCF7, female athymic nude mice	Frequency = 1.1 MHz, Peak negative pressure = 2.0 MPa, Duty cycle = 3000, Duration = 2.5 min	US-induced cavitation	• Cell killing was higher in MDA-MB-468 than MCF7 cells. • Increased tumor uptake by 66% in the MDA-MB-468 cell line.	[102]
Doxorubicin	Liposomes	Solid liver tumor (phase I clinical trial)	Frequency = 0.96 MHz, intensity and duration varied according to participant's predicted treatment plan	FUS-induced hyperthermia	• Mean difference between predicted and implemented treatment powers was 0.1 ± 17.7 W. • No evidence of focused US-related adverse effects.	[62]
Calcein	Albumin-Liposomes	Breast cancer cell lines (MDA-MB-231 and MCF-7)	Frequency = 20 kHz, Power density = 6, 7 and 12 W/cm^2, Frequency = 40 kHz, Power density = 1 W/cm^2	US-induced cavitation	• Calcein uptake by the cancer cells was enhanced following sonication.	[103]
Calcein	Emulsion-Liposomes (eLiposomes)	–	Frequency = 20 kHz, Power density = 5 W/cm^2	US-induced acoustic droplet vaporization (ADV)	• Following sonication, calcein release was significantly higher from eLiposomes compared to conventional liposomes.	[104]
Calcein	Estrone-Liposomes	Breast cancer cell lines MDA-MB-231 and MCF-7	Frequencies = 20 kHz, 1.07 and 3.24 MHz Power Density = varies	US-induced cavitation	• The exposure to LFUS revealed an enhanced calcein uptake by the cells.	[105]

Table I. Continued.

Drug loaded/contrast agent/model drug	Nanocarrier	Tumor model, Animal strain	Acoustic parameters	Mechanism of drug release	Main findings	Ref.
Calcein	Liposomes	–	Frequencies = 20 kHz 1, and 3 MHz, power density = varies	US-induced cavitation	• Calcein release was higher at the low frequency (20 kHz) investigated.	[106]
Doxorubicin	Folated eLiposomes (feLD)	KB-V1 (Dox resistant) and KB-3-1 (Dox sensitive) cell lines	Frequency = 20 kHz, Power Density = 1 W/cm^2	US-induced acoustic droplet vaporization (ADV)	• US released 78% of the encapsulated DOX from the feLD. US had no effect on the viability of both cell lines following the treatment with feLD.	[107]
Calcein	Emulsion-Liposomes (eLiposomes)	–	–	–	• Emulsion liposomes were found to be stable at room and physiological temperatures and released at 49 °C and 59 °C	[108]
Calcein	Emulsion-Liposomes (eLiposomes)	–	–	–	• The nucleation of gas is suspected as the prime mechanism in the passive (non-acoustic release from eLiposomes at 49 °C and 59 °C	[109]
Doxorubicin	Folated and non-folated Pluronic P105-micelles	–	Frequency = 70 kHz, Power Density = 0–0.8 W/cm^2	US-induced cavitation	• A cavitation model with Bayesian filters improves the prediction of the acoustic release of Doxorubicin from folated and non-folated micelles.	[110]
Calcein	Targeted Liposomes (Estrone-, Albumin-, RGD-Liposomes)	–	Frequency = 20 kHz, Power density = varies	US-induced cavitation	• First-order and Gompertz kinetic models gave the best fit to experimental release data. • An Adaptive Kalman Filter improved the fit of all five kinetic models employed.	[111]
Calcein	Targeted liposomes (Transferrin-, Albumin-, RGD-Liposomes)	–	Frequency = 20 kHz, Power density = 6, 7, and 12 W/cm^2	US-induced cavitation	• Pegylated liposomes were more sonosensitive compared to nonpegylated liposomes. • Albumin-PEG and Transferrin-PEG liposomes were more sonosensitive than non-targeted liposomes when exposed to LFUS.	[112]
Calcein	Liposomes	–	Frequency = 20 kHz, Power density = 6.08, 6.97, and 11.83 W/cm^2	US-induced cavitation	• A first-order kinetic model with an optimal Kalman filter adequately modeled calcein release from non-targeted liposomes when exposed to 20-kHz ultrasound.	[113]

Notes: *Abbreviations*: *DOX*, Doxorubicin; *PRF*, Pulse repetition frequency; *LFUS*, Low-frequency ultrasound; *HIFU*, High intensity focused ultrasound; *LIFU*, Low intensity focused ultrasound; *FUS*, Focused ultrasound; *TSL*, Thermo-sensitive liposomes; *NR*, Nile Red; *NCL*, Non-cross-linked; *CCL*, Core-cross-linked; *GSH*, Glutathione; *PEG-S-S-PLA*, Biodegradable block copolymer containing the central labile disulfide linkage between polyethylene glycol (PEG) and poly-l-lactic acid (PLA); *MDR*, Multi-drug resistant; *DTT*, Dithiothreitol; *PLA*, Poly(lactic acid); *ANN*, artificial neural networks; *eLiposomes*, emulsion-liposomes.

for drug delivery. This micelle system was composed of an amphiphilic copolymer, poly(ethylene oxide)-b-poly (N-isopropylacrylamide-co-2-hydroxyethyl methacrylate-lactate$_n$). The DOX release was about 2% at room temperature and 4% at body temperature, and the drug returned to the polymeric micelles when sonication ceased. Deckers et al. [65] investigated continuous wave (CW), HIFU-triggered payload release from non-cross-linked (NCL) and core cross-linked (CCL) poly(ethylene glycol)-b-poly[N-(2-hydroxypropyl)methacrylamide-lactate](mPEG-b-p(HPMAm-Lacn)) micelles. When sonicated, up to 85% Nile Red (NR) was released from both types of micelles. The researchers hypothesized that the release of NR from the micelles was caused by mechanical shear forces, and not due to cavitation.

The composition of the liposomal membrane has a significant effect on several properties, such as size, transition temperature, loading efficiency, and stability [1]. Several studies have shown that the lipid membrane constituents can affect the response of liposomes to sonication. Lin and Thomas [66] demonstrated that the inclusion of surfactants (Triton and Tween) and PEG, in conventional phosphatidylcholine (PC)-based liposomes, enhanced the *in vitro* drug release sonosensitivity. The authors attributed this enhanced effectiveness of insonation to ethylene oxide surfactants and lipids, which weakens the rupture tension of lipid membranes. Another proposed explanation is that US permeability differed in these liposome compositions because of differing kinetics in the evolution of an initial tear or pore. Evjen et al. [67] investigated the sonosensitivity of DOX-liposomes containing distearoylsn-glycero-3-phosphatidylethanolamine (DSPE). A variety of lipid bilayer compositions were studied in *in vitro* US triggered release of drugs, as well as serum stability. The optimal formulation, consisting of DSPE:DSPE-PEG:CHOL at a molar ratio of 62:8:30 mol%, showed approximately 70% release of DOX after 6 min of US exposure. This represented a 7-fold increase in release when compared to DSPC-based liposomes (DSPC:DSPE-PEG:CHOL at a molar ratio of 62:8:30 mol%). In another study by Evjen et al. [68], the effect of membrane composition on calcein release from dioleoylphosphatidylethanolamine (DOPE)-based liposomes upon exposure to 1.13 MHz focused US (FUS) was investigated. A strong correlation between sonosensitivity and the non-bilayer forming lipids DOPE and DSPE-PEG (2000) was demonstrated. All of the DOPE-based liposome formulations studied displayed both acceptable sonosensitivity and serum stability.

Therefore, the major parameters that affect US-induced liposomal drug release are lipid composition, the physical state of the bilayer, and the presence of PEG-moieties. Detergents and phospholipids with unsaturated acyl chains tend to disrupt the close packing structure of the lipid bilayer, hence increasing the liposomes' responsivity to US. These molecules seem to weaken the Vander Waal's forces between the acyl chains, thereby making the lipid bilayer more susceptible to the mechanical pressures induced by US. With regard to the physical state of the bilayer, the increased absorbance of ultrasonic energy by the lipid bilayer was shown to occur during the solid-ordered to liquid-disordered phase transition. Lastly, introducing PEG to the liposome membrane increases liposomal drug release [1, 69].

1.11. Effect of Ultrasound Parameters on Drug Release from Micelles and Liposomes

Several US parameters have been reported for the effective release of drugs from NPs; such parameters include frequency, negative pressure, amplitude, and duration. Husseini et al. [70] investigated the factors affecting acoustically-triggered drug release from polymeric micelles. The drug release from P-105 micelles was monitored using real-time fluorescence detection exposed to continuous wave or pulsed US in the frequency range of 20–90 kHz. Two fluorescent drugs were used, namely DOX and its paramagnetic counterpart Ruboxyl (Rb). The drug release was found to decrease with increasing frequency, indicating that transient cavitation has an essential role in drug release. The release of DOX was higher than that of Rb due to the deeper inclusion of Rb into the core of the micelles. At constant frequency, drug release increased with increasing power density; however, at a given power density, and for pulse durations longer than 0.1 s, the maximum release was the same as that under CW US. Marin et al. [71] studied the effect of CW and pulsed US on DOX uptake by human leukemia (HL-60) cells from a phosphate-buffered saline solution (PBS) and Pluronic® micellar solutions. The uptake of DOX was enhanced equally using both the CW and pulsed wave US insonation. The drug uptake also increased with increasing pulse duration in the range of 0.1–2 s. When using 2 s pulses, the uptake was similar to that under CW US. Additionally, a minimum threshold time value was established, as no significant drug release was observed when micelles were irradiated with a 20 kHz and 58 mW/cm^2 US beam for less than 0.1 s. Beyond this threshold, the amount of release was shown to increase as the pulse length increased up to 0.6 s. When exposed to US, micellar membranes were perturbed because of the shock waves produced by cavitational bubbles, inducing the release of hydrophobic drugs. Once the US treatment was halted, the micelles reassembled, and the drug molecules re-encapsulated.

In terms of the impact of US parameters on liposomal release, Afadzi et al. [72] investigated the manipulation of the aforementioned parameters to maximize the drug release from DEPC liposomes. The liposomes were exposed to FUS with frequencies of 300 kHz and 1 MHz, and a range of peak-negative pressures. At 300 kHz, the peak-negative pressure was varied from 0.29 to 1.7 MPa, whereas at 1 MHz, the peak-negative pressure varied from

0.68 to 3.58 MPa. The release of the model drug calcein was monitored by measuring the changes in fluorescence intensity with increasing acoustic pressure and exposure time. The spectrophotometric measurements showed that the release of calcein was more efficient at 300 kHz than at 1 MHz, even though the 1 MHz transducer was used at higher intensities and peak negative pressures. In order for the amount of drug release from liposomes to exceed 5%, the acoustic pressure had to exceed 0.9 MPa at 300 kHz (MI = 1.6), and 1.9 MPa at 1 MHz (MI = 1.9).

Additionally, the amount of drug release followed first-order kinetics and increased with exposure time until maxim release was achieved. The results of this study demonstrated that the MI and the overall exposure time are the major parameters that determine the extent of the drug release. Pong et al. [73] studied the effects of US frequency, amplitude, intensity and rate of drug delivery from phospholipid vesicles, having diameters of 100 nm, 300 nm, and 1 μm, and PEG concentrations of 2 mol%, 5 mol%, and 8 mol%, when exposed to US from plane and acoustic sources. Their experiments were performed at room temperature using a 20-kHz commercial transducer and two custom-built acoustic sources operating at frequencies of 1 MHz and 1.6 MHz. The results indicated that the release from vesicles could be enhanced by increasing the PEG concentration to 5 mol%, decreasing the membrane curvature, increasing the likelihood of transient cavitation by decreasing the frequency of the US source, and increasing the *On* time in order to facilitate the nucleation and growth of cavitation bubbles. In another study, Ahmed et al. [74] investigated the release of the model drug calcein from DOPE and DSPE liposomes exposed to 20 kHz LFUS at three power densities, and three On/Off pulse durations. The study concluded that when applying different pulses (10 s On/10 s Off, 20 s On/10 s *Off* and 20 s On/30 s Off), the only significant differences in release were obtained when the 'On' period is less or equal to the 'Off' period. With respect to power density, the experiments showed that release increased with increasing power density. Lastly, DSPE-liposomes were considerably more responsive to US than DOPE liposomes at the conditions investigated; this was attributed to the non-bilayer forming characteristics of saturated lipids (DSPE), which allow US to perturb the liposomal membrane more rigorously than when interacting with unsaturated layers.

2. CONCLUSION

We presented a review of US-induced drug release from both micelles and liposomes. The different US-mediated release mechanisms were addressed, as well as the membrane constituents and US parameters influencing ultrasonic drug release. Promising *in vitro* and *in vivo* results have been reported this past decade, and this proposed treatment has recently shown promise in clinical trials. This paper provided an overview of the body of literature pertaining to US responsive micelles and liposomes and detailed some relevant studies.

Acknowledgments: We acknowledge the financial support provided by the American University of Sharjah Faculty Research Grants, Dana Gas Endowed Chair for Chemical Engineering, Al-Jalila Foundation (AJF 2015555), Al Qasimi Foundation, Takamul, Technology Innovation Pioneer (TIP) Healthcare Awards, and Patient's Friends Committee-Sharjah.

References and Notes

1. Schroeder, A., Kost, J. and Barenholz, Y., **2009**. Ultrasound, liposomes, and drug delivery: principles for using ultrasound to control the release of drugs from liposomes. *Chemistry and Physics of Lipids*, *162*(1–2), pp.1–16.
2. Kane, D., Grassi, W., Sturrock, R. and Balint, P.V., **2004**. A brief history of musculoskeletal ultrasound: 'From bats and ships to babies and hips'. *Rheumatology*, *43*(7), pp.931–933.
3. Muir, T.G. and Bradley, D.L., **2016**. Underwater acoustics: A brief historical overview through world war II. *Acoustics Today*, *12*(3).
4. Newman, P.G. and Rozycki, G.S., **1998**. The history of ultrasound. *Surgical Clinics of North America*, *78*(2), pp.179–195.
5. Smagulova, D. and Jasiuniene, E., **2018**. Inspection of Dissimilar Material Joints Using Ultrasonic Phased Arrays. *Elektronika ir Elektrotechnika*, *24*(6), pp.28–32.
6. Amplitude, Britannica.com (https://www.britannica.com/science/amplitude-physics).
7. Coltrera, M.D., **2010**. Ultrasound physics in a nutshell. *Otolaryngologic Clinics of North America*, *43*(6), pp.1149–1159.
8. Martins, A.M., Elgaili, S.A., Vitor, R.F. and Husseini, G.A., **2016**. Ultrasonic drug delivery using micelles and liposomes. *Handbook of Ultrasonics and Sonochemistry*, pp.1127–1161.
9. Smith, N.B. and Webb, A., **2010**. *Introduction to Medical Imaging: Physics, Engineering and Clinical Applications*. Cambridge University Press.
10. Webster, J.G. ed., **2009**. *Medical Instrumentation: Application and Design*. John Wiley & Sons.
11. How Ultrasonic Waves Are Generated (https://science.jrank.org/pages/7075/Ultrasonics-How-ultrasonic-waves-are-generated.html).
12. Ultrasound (https://www.nibib.nih.gov/science-education/science-topics/ultrasound).
13. Kondo, T., **2015**. Application of ultrasound in medicine and biotechnology. In *Sonochemistry and the Acoustic Bubble*. Elsevier. pp.207–230.
14. Miller, D.L., Smith, N.B., Bailey, M.R., Czarnota, G.J., Hynynen, K., Makin, I.R.S. and Bioeffects committee of the american institute of ultrasound in medicine, **2012**. Overview of therapeutic ultrasound applications and safety considerations. *Journal of Ultrasound in Medicine*, *31*(4), pp.623–634.
15. Azagury, A., Khoury, L., Enden, G. and Kost, J., **2014**. Ultrasound mediated transdermal drug delivery. *Advanced Drug Delivery Reviews*, *72*, pp.127–143.
16. Frenkel, V., **2008**. Ultrasound mediated delivery of drugs and genes to solid tumors. *Advanced Drug Delivery Reviews*, *60*(10), pp.1193–1208.
17. Cheng, X., Zhang, M., Xu, B., Adhikari, B. and Sun, J., **2015**. The principles of ultrasound and its application in freezing related processes of food materials: A review. *Ultrasonics Sonochemistry*, *27*, pp.576–585.
18. Richardson, E.S., Pitt, W.G. and Woodbury, D.J., **2007**. The role of cavitation in liposome formation. *Biophysical Journal*, *93*(12), pp.4100–4107.

19. Baykal-Caglar, E., Hassan-Zadeh, E., Saremi, B. and Huang, J., **2012**. Preparation of giant unilamellar vesicles from damp lipid film for better lipid compositional uniformity. *Biochimica et Biophysica Acta (BBA)-Biomembranes*, *1818*(11), pp.2598–2604.

20. Tuziuti, T., Yasui, K., Lee, J., Kozuka, T., Towata, A. and Iida, Y., **2008**. Mechanism of enhancement of sonochemical-reaction efficiency by pulsed ultrasound. *The Journal of Physical Chemistry A*, *112*(22), pp.4875–4878.

21. Xia, H., Zhao, Y. and Tong, R., **2016**. Ultrasound-mediated polymeric micelle drug delivery. In *Therapeutic Ultrasound*. Springer, Cham. pp.365–384.

22. Seema, R., Chanchal, C., Ravi, S., Ankur, R., Dinesh, K., Satish, S. and Harish, D., **2012**. Liposomes: Preparations and applications. *Int. J. Drug. Dev. Res*, *4*(4), pp.108–115.

23. Cartaxo, A.L.P., **2010**. Nanoparticles types and properties–understanding these promising devices in the biomedical area.

24. Bhatia, S., **2016**. Nanoparticles types, classification, characterization, fabrication methods and drug delivery applications. In *Natural Polymer Drug Delivery Systems*. Springer, Cham. pp.33–93.

25. Grigore, M.E., **2017**. Organic and inorganic nano-systems used in cancer treatment. *Journal of Medical Research and Health Education*, *1*(3).

26. Moreno-Vega, A.I., Gomez-Quintero, T., Nunez-Anita, R.E., Acosta-Torres, L.S. and Castaño, V., **2012**. Polymeric and ceramic nanoparticles in biomedical applications. *Journal of Nanotechnology*.

27. Daraee, H., Etemadi, A., Kouhi, M., Alimirzalu, S. and Akbarzadeh, A., **2016**. Application of liposomes in medicine and drug delivery. *Artificial Cells, Nanomedicine, and Biotechnology*, *44*(1), pp.381–391.

28. Chang, H.I. and Yeh, M.K., **2012**. Clinical development of liposome-based drugs: Formulation, characterization, and therapeutic efficacy. *International Journal of Nanomedicine*, *7*, p.49.

29. van Rooijen, N., **1998**. Liposomes. *Encycl. Immunol.,* pp.1588–1592.

30. PHILPOT EDUCATION, The origin of cells, (https://www.philpoteducation.com/mod/book/view.php?id=777&chapterid=1121#/).

31. Silindir-Gunay, M. and Ozer, A.Y., **2018**. Liposomes and micelles as nanocarriers for diagnostic and imaging purposes. In *Design of Nanostructures for Theranostics Applications*. William Andrew Publishing. pp.305–340.

32. Khan, Y.Y. and Suvarna, V., **2017**. Liposomes containing phytochemicals for cancer treatment-an update. *Int. J. Curr. Pharm. Rev. Res*, *9*(1), pp.20–24.

33. Akbarzadeh, A., Rezaei-Sadabady, R., Davaran, S., Joo, S.W., Zarghami, N., Hanifehpour, Y., Samiei, M., Kouhi, M. and Nejati-Koshki, K., **2013**. Liposome: Classification, preparation, and applications. *Nanoscale Research Letters*, *8*(1), p.102.

34. Nag, O.K. and Awasthi, V., **2013**. Surface engineering of liposomes for stealth behavior. *Pharmaceutics*, *5*(4), pp.542–569.

35. Immordino, M.L., Dosio, F. and Cattel, L., **2006**. Stealth liposomes: Review of the basic science, rationale, and clinical applications, existing and potential. *International Journal of Nanomedicine*, *1*(3), p.297.

36. Drabu, S., Khanna, S., Bajaj, R. and Khurana, B., **2010**. Clinical pharmacokinetic aspects of stealth liposomes: A review. *Int. J. Drug Dev. Res.*, *2*, pp.871–878.

37. Moghimi, S.M. and Szebeni, J., **2003**. Stealth liposomes and long circulating nanoparticles: Critical issues in pharmacokinetics, opsonization and protein-binding properties. *Progress in Lipid Research*, *42*(6), pp.463–478.

38. Allen, C.D.S.N., Dos Santos, N., Gallagher, R., Chiu, G.N.C., Shu, Y., Li, W.M., Johnstone, S.A., Janoff, A.S., Mayer, L.D., Webb, M.S. and Bally, M.B., **2002**. Controlling the physical behavior and biological performance of liposome formulations through use of surface grafted poly (ethylene glycol). *Bioscience Reports*, *22*(2), pp.225–250.

39. Moghimi, S.M., Hunter, A.C. and Murray, J.C., **2001**. Long-circulating and target-specific nanoparticles: Theory to practice. *Pharmacological Reviews*, *53*(2), pp.283–318.

40. Chowdhury, S.M., Lee, T. and Willmann, J.K., **2017**. Ultrasound-guided drug delivery in cancer. *Ultrasonography*, *36*(3), p.171.

41. Vincent, B., **2014**. McBain and the centenary of the micelle. *Advances in Colloid and Interface Science*, *203*, pp.51–54.

42. Fujii, S., Yamada, S., Matsumoto, S., Kubo, G., Yoshida, K., Tabata, E., Miyake, R., Sanada, Y., Akiba, I., Okobira, T. and Yagi, N., **2017**. Platonic micelles: Monodisperse micelles with discrete aggregation numbers corresponding to regular polyhedra. *Scientific Reports*, *7*, p.44494.

43. Attwood, D. and Saunders, L., **1965**. A light-scattering study of ultrasonically irradiated lecithin sols. *Biochimica et Biophysica Acta (BBA)-Lipids and Lipid Metabolism*, *98*(2), pp.344–350.

44. Papahadjopoulos, D. and Miller, N., **1967**. Phospholipid model membranes. I. Structural characteristics of hydrated liquid crystals. *Biochimica et Biophysica Acta (BBA)-Biomembranes*, *135*(4), pp.624–638.

45. Papahadjopoulos, D. and Watkins, J.C., **1967**. Phospholipid model membranes. II. Permeability properties of hydrated liquid crystals. *Biochimica et Biophysica Acta (BBA)-Biomembranes*, *135*(4), pp.639–652.

46. Huang, C.H., **1969**. Phosphatidylcholine vesicles. Formation and physical characteristics. *Biochemistry*, *8*(1), pp.344–352.

47. Tejera-Garcia, R., Ranjan, S., Zamotin, V., Sood, R. and Kinnunen, P.K., **2011**. Making unilamellar liposomes using focused ultrasound. *Langmuir*, *27*(16), pp.10088–10097.

48. Vemuri, S. and Rhodes, C.T., **1995**. Preparation and characterization of liposomes as therapeutic delivery systems: A review. *Pharmaceutica Acta Helvetiae*, *70*(2), pp.95–111.

49. Schroeder, A., Avnir, Y., Weisman, S., Najajreh, Y., Gabizon, A., Talmon, Y., Kost, J. and Barenholz, Y., **2007**. Controlling liposomal drug release with low frequency ultrasound: Mechanism and feasibility. *Langmuir*, *23*(7), pp.4019–4025.

50. Soga, O., van Nostrum, C.F., Fens, M., Rijcken, C.J., Schiffelers, R.M., Storm, G. and Hennink, W.E., **2005**. Thermosensitive and biodegradable polymeric micelles for paclitaxel delivery. *Journal of Controlled Release*, *103*(2), pp.341–353.

51. Li, M., Xiao, X., Zhang, W., Liu, L., Xi, N. and Wang, Y., **2014**. Nanoscale distribution of CD20 on B-cell lymphoma tumour cells and its potential role in the clinical efficacy of rituximab. *Journal of Microscopy*, *254*(1), pp.19–30.

52. Karimi, M., Ghasemi, A., Zangabad, P.S., Rahighi, R., Basri, S.M.M., Mirshekari, H., Amiri, M., Pishabad, Z.S., Aslani, A., Bozorgomid, M. and Ghosh, D., **2016**. Smart micro/nanoparticles in stimulus-responsive drug/gene delivery systems. *Chemical Society Reviews*, *45*(5), pp.1457–1501.

53. Rapoport, N., **2012**. Ultrasound-mediated micellar drug delivery. *International Journal of Hyperthermia*, *28*(4), pp.374–385.

54. Munshi, N., Rapoport, N. and Pitt, W.G., **1997**. Ultrasonic activated drug delivery from Pluronic P-105 micelles. *Cancer Letters*, *118*(1), pp.13–19.

55. Husseini, G.A., Velluto, D., Kherbeck, L., Pitt, W.G., Hubbell, J.A. and Christensen, D.A., **2013**. Investigating the acoustic release of doxorubicin from targeted micelles. *Colloids and Surfaces B: Biointerfaces*, *101*, pp.153–155.

56. Stevenson-Abouelnasr, D., Husseini, G.A. and Pitt, W.G., **2007**. Further investigation of the mechanism of Doxorubicin release from P105 micelles using kinetic models. *Colloids and Surfaces B: Biointerfaces*, *55*(1), pp.59–66.

57. Xuan, J., Pelletier, M., Xia, H. and Zhao, Y., **2011**. Ultrasound-induced disruption of amphiphilic block copolymer micelles. *Macromolecular Chemistry and Physics*, *212*(5), pp.498–506.

58. Tacker, J.R. and Anderson, R.U., **1982**. Delivery of antitumor drug to bladder cancer by use of phase transition liposomes and hyperthermia. *The Journal of Urology*, *127*(6), pp.1211–1214.

59. Ning, S., Macleod, K., Abra, R.M., Huang, A.H. and Hahn, G.M., **1994**. Hyperthermia induces doxorubicin release from long-circulating liposomes and enhances their anti-tumor efficacy. *International Journal of Radiation Oncology∗ Biology∗ Physics*, *29*(4), pp.827–834.

60. Lafon, C., Somaglino, L., Bouchoux, G., Mari, J.M., Chesnais, S., Ngo, J., Mestas, J.L., Fossheim, S.L., Nilssen, E.A. and Chapelon, J.Y., **2012**. Feasibility study of cavitation-induced liposomal doxorubicin release in an AT2 Dunning rat tumor model. *Journal of Drug Targeting*, *20*(8), pp.691–702.

61. Mannaris, C., Efthymiou, E., Meyre, M.E. and Averkiou, M.A., **2013**. In vitro localized release of thermosensitive liposomes with ultrasound-induced hyperthermia. *Ultrasound in Medicine & Biology*, *39*(11), pp.2011–2020.

62. Gray, M.D., Lyon, P.C., Mannaris, C., Folkes, L.K., Stratford, M., Campo, L., Chung, D.Y.F., Scott, S., Anderson, M., Goldin, R., Carlisle, R., Wu, F., Middleton, M.R., Gleeson, F.V. and Coussios, C.C., **2019**. *Radiology, 291*, p.232.

63. Rapoport, N., **1999**. Stabilization and activation of Pluronic micelles for tumor-targeted drug delivery. *Colloids and Surfaces B: Biointerfaces*, *16*(1–4), pp.93–111.

64. Zeng, Y. and Pitt, W.G., **2006**. A polymeric micelle system with a hydrolysable segment for drug delivery. *Journal of Biomaterials Science, Polymer Edition*, *17*(5), pp.591–604.

65. Deckers, R., Paradissis, A., Oerlemans, C., Talelli, M., Storm, G., Hennink, W.E. and Nijsen, J.F.W., **2013**. New insights into the HIFU-triggered release from polymeric micelles. *Langmuir*, *29*(30), pp.9483–9490.

66. Lin, H.Y. and Thomas, J.L., **2003**. Peg–lipids and oligo (ethylene glycol) surfactants enhance the ultrasonic permeabilizability of liposomes. *Langmuir*, *19*(4), pp.1098–1105.

67. Evjen, T.J., Nilssen, E.A., Rögnvaldsson, S., Brandl, M. and Fossheim, S.L., **2010**. Distearoylphosphatidylethanolamine-based liposomes for ultrasound-mediated drug delivery. *European Journal of Pharmaceutics and Biopharmaceutics*, *75*(3), pp.327–333.

68. Evjen, T.J., Nilssen, E.A., Fowler, R.A., Røgnvaldsson, S., Brandl, M. and Fossheim, S.L., **2011**. Lipid membrane composition influences drug release from dioleoylphosphatidylethanolamine-based liposomes on exposure to ultrasound. *International Journal of Pharmaceutics*, *406*(1–2), pp.114–116.

69. Barenholz, Y., **2001**. Liposome application: Problems and prospects. *Current Opinion in Colloid & Interface Science*, *6*(1), pp.66–77.

70. Husseini, G.A., Myrup, G.D., Pitt, W.G., Christensen, D.A. and Rapoport, N.Y., **2000**. Factors affecting acoustically triggered release of drugs from polymeric micelles. *Journal of Controlled Release*, *69*(1), pp.43–52.

71. Marin, A., Muniruzzaman, M. and Rapoport, N., **2001**. Acoustic activation of drug delivery from polymeric micelles: Effect of pulsed ultrasound. *Journal of Controlled Release*, *71*(3), pp.239–249.

72. Afadzi, M., Davies, C.D.L., Hansen, Y.H., Johansen, T., Standal, Ø.K., Hansen, R., Måsøy, S.E., Nilssen, E.A. and Angelsen, B., **2012**. Effect of ultrasound parameters on the release of liposomal calcein. *Ultrasound in Medicine & Biology*, *38*(3), pp.476–486.

73. Pong, M., Umchid, S., Guarino, A.J., Lewin, P.A., Litniewski, J., Nowicki, A. and Wrenn, S.P., **2006**. In vitro ultrasound-mediated leakage from phospholipid vesicles. *Ultrasonics*, *45*(1–4), pp.133–145.

74. Ahmed, S.E., Moussa, H.G., Martins, A.M., Abbas, Y., Al-Sayah, M.H. and Husseini, G.A., **2019**. Factors affecting the acoustic in vitro release of calcein from PEGylated liposomes. *Journal of Nanoscience and Nanotechnology*, *19*(11), pp.6899–6906.

75. Nelson, J.L., Roeder, B.L., Carmen, J.C., Roloff, F. and Pitt, W.G., **2002**. Ultrasonically activated chemotherapeutic drug delivery in a rat model. *Cancer Research*, *62*(24), pp.7280–7283.

76. Marin, A., Sun, H., Husseini, G.A., Pitt, W.G., Christensen, D.A. and Rapoport, N.Y., **2002**. Drug delivery in pluronic micelles: Effect of high-frequency ultrasound on drug release from micelles and intracellular uptake. *Journal of Controlled Release*, *84*(1–2), pp.39–47.

77. Husseini, G.A., de la Rosa, M.A.D., Richardson, E.S., Christensen, D.A. and Pitt, W.G., **2005**. The role of cavitation in acoustically activated drug delivery. *Journal of Controlled Release*, *107*(2), pp.253–261.

78. Myhr, G. and Moan, J., **2006**. Synergistic and tumour selective effects of chemotherapy and ultrasound treatment. *Cancer letters*, *232*(2), pp.206–213.

79. Dromi, S., Frenkel, V., Luk, A., Traughber, B., Angstadt, M., Bur, M., Poff, J., Xie, J., Libutti, S.K., Li, K.C. and Wood, B.J., **2007**. Pulsed-high intensity focused ultrasound and low temperature—Sensitive liposomes for enhanced targeted drug delivery and antitumor effect. *Clinical Cancer Research*, *13*(9), pp.2722–2727.

80. Husseini, G.A., Diaz de la Rosa, M.A., Gabuji, T., Zeng, Y., Christensen, D.A. and Pitt, W.G., **2007**. Release of doxorubicin from unstabilized and stabilized micelles under the action of ultrasound. *Journal of Nanoscience and Nanotechnology*, *7*(3), pp.1028–1033.

81. Smith, M.J., Eccleston, M.E. and Slater, N.K., **2008**. The effect of high intensity focussed ultrasound (HIFU) on pH responsive PEGylated micelles. *Journal of the Acoustical Society of America*, *123*(5), p.3223.

82. Ugarenko, M., Chan, C.K., Nudelman, A., Rephaeli, A., Cutts, S.M. and Phillips, D.R., **2009**. Development of pluronic micelle-encapsulated doxorubicin and formaldehyde-releasing prodrugs for localized anticancer chemotherapy. *Oncology Research Featuring Preclinical and Clinical Cancer Therapeutics*, *17*(7), pp.283–299.

83. Zhang, H., Xia, H., Wang, J. and Li, Y., **2009**. High intensity focused ultrasound-responsive release behavior of PLA-b-PEG copolymer micelles. *Journal of Controlled Release*, *139*(1), pp.31–39.

84. Husseini, G.A., Mjalli, F.S., Pitt, W.G. and Abdel-Jabbar, N.M., **2009**. Using artificial neural networks and model predictive control to optimize acoustically assisted doxorubicin release from polymeric micelles. *Technology in Cancer Research & Treatment*, *8*(6), pp.479–488.

85. Schroeder, A., Honen, R., Turjeman, K., Gabizon, A., Kost, J. and Barenholz, Y., **2009**. Ultrasound triggered release of cisplatin from liposomes in murine tumors. *Journal of Controlled Release*, *137*(1), pp.63–68.

86. Li, Y., Tong, R., Xia, H., Zhang, H. and Xuan, J., **2010**. High intensity focused ultrasound and redox dual responsive polymer micelles. *Chemical Communications*, *46*(41), pp.7739–7741.

87. Negussie, A.H., Yarmolenko, P.S., Partanen, A., Ranjan, A., Jacobs, G., Woods, D., Bryant, H., Thomasson, D., Dewhirst, M.W., Wood, B.J. and Dreher, M.R., **2011**. Formulation and characterisation of magnetic resonance imageable thermally sensitive liposomes for use with magnetic resonance-guided high intensity focused ultrasound. *International Journal of Hyperthermia*, *27*(2), pp.140–155.

88. Pitt, W.G., Husseini, G.A., Roeder, B.L., Dickinson, D.J., Warden, D.R., Hartley, J.M. and Jones, P.W., **2011**. Preliminary results of combining low frequency low intensity ultrasound and liposomal drug delivery to treat tumors in rats. *Journal of Nanoscience and Nanotechnology*, *11*(3), pp.1866–1870.

89. Hasanzadeh, H., Mokhtari-Dizaji, M., Bathaie, S.Z. and Hassan, Z.M., **2011**. Effect of local dual frequency sonication on drug distribution from polymeric nanomicelles. *Ultrasonics Sonochemistry*, *18*(5), pp.1165–1171.

90. Kobayashi, D., Karasawa, M., Takahashi, T., Otake, K. and Shono, A., **2012**. Effluence of internal substances from pluronic micelle using ultrasound. *Japanese Journal of Applied Physics*, *51*(7S), p.07GD10.

91. Aryal, M., Vykhodtseva, N., Zhang, Y.Z., Park, J. and McDannold, N., **2013**. Multiple treatments with liposomal doxorubicin and ultrasound-induced disruption of blood–tumor and blood–brain barriers improve outcomes in a rat glioma model. *Journal of Controlled Release*, *169*(1–2), pp.103–111.

92. Tong, R., Xia, H. and Lu, X., **2013**. Fast release behavior of block copolymer micelles under high intensity focused ultrasound/redox combined stimulus. *Journal of Materials Chemistry B*, *1*(6), pp.886–894.

93. Maples, D., McLean, K., Sahoo, K., Newhardt, R., Venkatesan, P., Wood, B. and Ranjan, A., **2015**. Synthesis and characterisation of ultrasound imageable heat-sensitive liposomes for HIFU therapy. *International Journal of Hyperthermia*, *31*(6), pp.674–685.

94. Hijnen, N., Kneepkens, E., de Smet, M., Langereis, S., Heijman, E. and Grüll, H., **2017**. Thermal combination therapies for local drug delivery by magnetic resonance-guided high-intensity focused ultrasound. *Proceedings of the National Academy of Sciences*, *114*(24), pp.E4802–E4811.

95. Ektate, K., Munteanu, M.C., Ashar, H., Malayer, J. and Ranjan, A., **2018**. Chemo-immunotherapy of colon cancer with focused ultrasound and Salmonella-laden temperature sensitive liposomes (thermobots). *Scientific Reports*, *8*(1), p.13062.

96. Wadi, A., Abdel-Hafez, M. and Husseini, G.A., **2017**. Identification of the uncertainty structure to estimate the acoustic release of chemotherapeutics from polymeric micelles. *IEEE Transactions on Nanobioscience*, *16*(7), pp.609–617.

97. Lin, Q., Mao, K.L., Tian, F.R., Yang, J.J., Chen, P.P., Xu, J., Fan, Z.L., Zhao, Y.P., Li, W.F., Zheng, L. and Zhao, Y.Z., **2016**. Brain tumor-targeted delivery and therapy by focused ultrasound introduced doxorubicin-loaded cationic liposomes. *Cancer Chemotherapy and Pharmacology*, *77*(2), pp.269–280.

98. Deng, Z., Xiao, Y., Pan, M., Li, F., Duan, W., Meng, L., Liu, X., Yan, F. and Zheng, H., **2016**. Hyperthermia-triggered drug delivery from iRGD-modified temperature-sensitive liposomes enhances the anti-tumor efficacy using high intensity focused ultrasound. *Journal of Controlled Release*, *243*, pp.333–341.

99. Martins, A.M., Tanbour, R., Elkhodiry, M.A. and Husseini, G.A., **2016**. Ultrasound-induced doxorubicin release from folate-targeted and non-targeted P105 micelles: A modeling study. *European Journal of Nanomedicine*, *8*(1), pp.17–29.

100. Papachristodoulou, A., Signorell, R.D., Werner, B., Brambilla, D., Luciani, P., Cavusoglu, M., Grandjean, J., Silginer, M., Rudin, M., Martin, E. and Weller, M., **2019**. Chemotherapy sensitization of glioblastoma by focused ultrasound-mediated delivery of therapeutic liposomes. *Journal of Controlled Release*, *295*, pp.130–139.

101. Camus, M., Vienne, A., Mestas, J.L., Pratico, C., Nicco, C., Chereau, C., Marie, J.M., Moussatov, A., Renault, G., Batteux, F. and Lafon, C., **2019**. Cavitation-induced release of liposomal chemotherapy in orthotopic murine pancreatic cancer models: A feasibility study. *Clinics and Research in Hepatology and Gastroenterology*.

102. Thomas, E., Menon, J.U., Owen, J., Skaripa-Koukelli, I., Wallington, S., Gray, M., Mannaris, C., Kersemans, V., Allen, D., Kinchesh, P. and Smart, S., **2019**. Ultrasound-mediated cavitation enhances the delivery of an EGFR-targeting liposomal formulation designed for chemo-radionuclide therapy. *Theranostics*, *9*(19), p.5595.

103. Awad, N.S., Paul, V., Al-Sayah, M.H. and Husseini, G.A., **2019**. Ultrasonically controlled albumin-conjugated liposomes for breast cancer therapy. *Artificial Cells, Nanomedicine, and Biotechnology*, *47*(1), pp.705–714.

104. Lattin, J.R., Pitt, W.G., Belnap, D.M. and Husseini, G.A., **2012**. Ultrasound-induced calcein release from eLiposomes. *Ultrasound in Medicine & Biology*, *38*(12), pp.2163–2173.

105. Salkho, N.M., Paul, V., Kawak, P., Vitor, R.F., Martins, A.M., Al Sayah, M. and Husseini, G.A., **2018**. Ultrasonically controlled estrone-modified liposomes for estrogen-positive breast cancer therapy. *Artificial Cells, Nanomedicine, and Biotechnology*, *46*(Suppl.2), pp.462–472.

106. Ahmed, S.E., Moussa, H.G., Martins, A.M., Al-Sayah, M.H. and Husseini, G.A., **2016**. Effect of pH, ultrasound frequency and power density on the release of calcein from stealth liposomes. *European Journal of Nanomedicine*, *8*(1), pp.31–43.

107. Williams, J.B., Buchanan, C.M., Husseini, G. and Pitt, W.G., **2017**. Cytosolic delivery of doxorubicin from liposomes to multidrug-resistant cancer cells via vaporization of perfluorocarbon droplets. *J. Nanomed. Res.*, *5*(4), p.00122.

108. Husseini, G.A., Pitt, W.G., Williams, J.B. and Javadi, M., **2014**. Investigating the release mechanism of calcein from eliposomes at higher temperatures. *Journal of Colloid Science and Biotechnology*, *3*(3), pp.239–244.

109. Husseini, G.A., Pitt, W.G. and Javadi, M., **2015**. Investigating the stability of eliposomes at elevated temperatures. *Technology in Cancer Research & Treatment*, *14*(4), pp.379–382.

110. Abusara, A., Abdel-Hafez, M. and Husseini, G., **2018**. Measuring the acoustic release of a chemotherapeutic agent from folate-targeted polymeric micelles. *Journal of Nanoscience and Nanotechnology*, *18*(8), pp.5511–5519.

111. Wadi, A., Abdel-Hafez, M., Husseini, G.A. and Paul, V., **2019**. Multi-model investigation and adaptive estimation of the acoustic release of a model drug from liposomes. *IEEE Transactions on Nanobioscience*.

112. Awad, N., Paul, V., Mahmoud, M., Al Sawaftah, N., Kawak, P., Al-Sayah, M.H. and Husseini, G.A., **2019**. The effect of pegylation and targeting moieties on the ultrasound-mediated drug release from liposomes. *ACS Biomaterials Science & Engineering*.

113. Wadi, A., Abdel-Hafez, M. and Husseini, G.A., **2019**. Modeling and bias-robust estimation of the acoustic release of chemotherapeutics from liposomes. *Journal of Biomedical Nanotechnology*, *15*(1), pp.162–169.

Received: 5 December 2019. Accepted: 22 April 2020.